

## Correction of node mapping distortions using universal serendipity elements in dynamical problems

Semih Küçükarslan\*<sup>1</sup> and Ali Demir<sup>2</sup>

<sup>1</sup>Department of Civil Engineering, İstanbul Technical University, Maslak, İstanbul, Turkey

<sup>2</sup>Department of Civil Engineering, Celal Bayar University, Manisa, Turkey

(Received December 10, 2010, Revised July 20, 2011, Accepted August 17, 2011)

**Abstract.** In this paper, the use of universal serendipity elements (USE) to eliminate node mapping distortions for dynamic problem is presented. Rectangular shaped elements for USE are being introduced by using a flexible master element with an adjustable edge node location. The shape functions of the universal serendipity formulation are used to derive the mass and damping matrices for the dynamic analyses. These matrices eliminate the node mapping distortion errors that occurs incase of the standard shape function formulations. The verification of new formulation will be tested and the errors encountered in the standard formulation will be studied for a dynamically loaded deep cantilever.

**Keywords:** finite element method; universal serendipity element (USE); node mapping distortion; dynamic analysis

---

### 1. Introduction

The order of an element in the finite element method is very important when higher accuracy is required although the computation time increases. From the Lagrange elements to the serendipity elements, many researches were performed to increase the level of accuracy in the obtained results. That is especially important for the stress concentration zones in the solid mechanics problems.

For the finite element analysis, the serendipity types of elements are constructed for the rectangular shapes. The procedure of the formulation of serendipity elements requires a mapping between a master element of simple shape and a physical element in global space. The physical location of edge nodes on physical element affects the mapping process since they are conventionally mapped to fixed locations on the master element. If the edge nodes of the physical element are mis-positioned, this results in a distortion which causes the polynomial functions in the master element to be mapped into transcendental functions in global space (Nicolas and Çıtıptıoğlu 1977), Fig. 1. This figure shows the mapping of a physical element to master element.

To eliminate mapping distortions, a flexible master element was improved in the previous studies, (Çıtıptıoğlu 1983, Celia and Cray 1984, Utku *et al.* 1991, Küçükarslan 1995, Utku 2000). A modification of the 8-node serendipity element was done by Kikuchi *et al.* (1999). Another study to

---

\*Corresponding author, Professor, E-mail: [kucukarslan@itu.edu.tr](mailto:kucukarslan@itu.edu.tr)

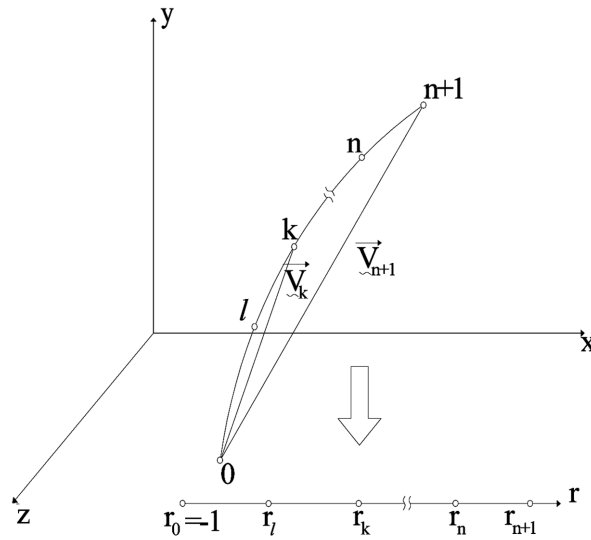


Fig. 1 Mapping of physical coordinates to master element

improve accuracy of finite element analysis was performed by Ho and Yeh (2006) by enriching master elements with addition of interior nodal points. The research conducted in Dhananjaya *et al.* (2009) and Dhananjaya *et al.* (2010) was mainly focused for plate elements.

Due to some structural engineering problems (El-mezaini and Çıtırıtıoğlu 1991, Heng and Mackie 2009, Konstantinos 2009, Chamberland *et al.* 2010, Lim *et al.* 2010), the edge points need to be located not exactly on the mid points of the master element. Since universal serendipity elements are capable of elimination of node mapping distortions with flexible edge node locations and also they are allow the use of different order of elements without using a constraint condition, they are highly desirable for higher accuracy and lower computation effort in the finite element analyses (Utku 2000).

A generalization of the concept of the universal serendipity elements is presented first time by introducing a more flexible master element with adjustable edge node locations for dynamical problems. With this innovative work, an extensive gap of mapping distortions in dynamical problems was eliminated. For this purpose, the mass and damping matrices will be derived and a deep cantilever beam will be studied as a numerical example. The verification of the new approach will be done and then the comparisons will be done with the standard formulations to see the distortion effect in the results. In this paper, the “standard formulation” term is used for the formulation of the shape functions when the mid-point is exactly at the center of the edge.

## 2. Formulation of shape functions for USE

The shape function formulation for the universal elements was given by Küçükarslan (1995) and Utku (2000) as in the following form (Fig. 2).

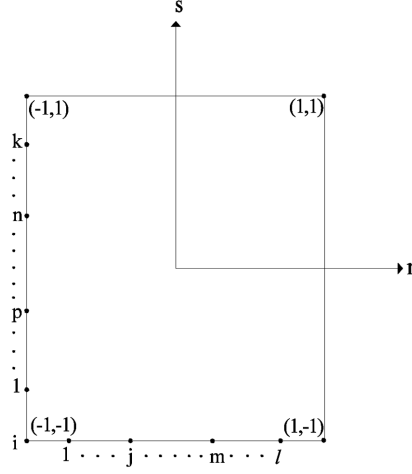


Fig. 2 A flexible master element

i) Shape function for any corner node  $i$

$$N_i(r, s) = \frac{(1+r_i r)(1+s_i s)}{4} \left[ \prod_{\substack{m=1 \\ |r_m| \neq 1}}^{\ell} \frac{r-r_m}{r_i-r_m} + \prod_{\substack{n=1 \\ |s_n| \neq 1}}^k \frac{s-s_n}{s_i-s_n} - 1 \right] \quad (1)$$

ii) Shape function for any nodal point  $m$  parallel to  $r$ -axis

$$N_m(r, s) = \frac{(r^2-1)(1+s_m s)}{2(r_m^2-1)} \left[ \prod_{\substack{j=1 \\ j \neq m, |r_j| \neq 1}}^{\ell} \frac{r-r_j}{r_m-r_j} \right] \quad (2)$$

iii) Shape function for any nodal point  $n$  parallel to  $s$ -axis

$$N_n(r, s) = \frac{(s^2-1)(1+r_n r)}{2(s_n^2-1)} \left[ \prod_{\substack{p=1 \\ p \neq n, |s_p| \neq 1}}^k \frac{s-s_p}{s_n-s_p} \right] \quad (3)$$

For a quadratic universal serendipity element with flexible midpoints (Fig. 3), Eqs. (1)-(3) reduce to the following forms

$$N_1(r, s, r_1, s_1) = \frac{(1-r)(1-s)}{4} \left( \frac{r_1-\alpha}{-1-\alpha} + \frac{s_1-\varepsilon}{-1-\varepsilon} - 1 \right) \quad (4)$$

$$N_2(r, s, r_2, s_2) = \frac{(1+r)(1-s)}{4} \left( \frac{r_2-\alpha}{1-\alpha} + \frac{s_2-\beta}{-1-\beta} - 1 \right) \quad (5)$$

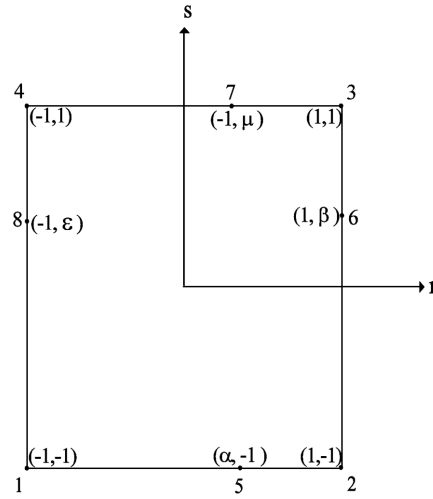


Fig. 3 USE with flexible midpoints

$$N_3(r, s, r_3, s_3) = \frac{(1+r)(1+s)}{4} \left( \frac{r_3 - \mu}{1 - \mu} + \frac{s_3 - \beta}{1 - \beta} - 1 \right) \tag{6}$$

$$N_4(r, s, r_4, s_4) = \frac{(1-r)(1+s)}{4} \left( \frac{r_4 - \mu}{-1 - \mu} + \frac{s_4 - \epsilon}{1 - \epsilon} - 1 \right) \tag{7}$$

$$N_5(r, s) = \begin{cases} \frac{(r^2 - 1)(1 - s)}{2(\alpha^2 - 1)}, & \text{if } \alpha \neq 1 \\ 0, & \text{if } \alpha = 1 \end{cases} \tag{8}$$

$$N_6(r, s) = \begin{cases} \frac{(s^2 - 1)(1 + r)}{2(\beta^2 - 1)}, & \text{if } \beta \neq 1 \\ 0, & \text{if } \beta = 1 \end{cases} \tag{9}$$

$$N_7(r, s) = \begin{cases} \frac{(r^2 - 1)(1 + s)}{2(\mu^2 - 1)}, & \text{if } \mu \neq 1 \\ 0, & \text{if } \mu = 1 \end{cases} \tag{10}$$

$$N_8(r, s) = \begin{cases} \frac{(s^2 - 1)(1 - r)}{2(\epsilon^2 - 1)}, & \text{if } \epsilon \neq 1 \\ 0, & \text{if } \epsilon = 1 \end{cases} \tag{11}$$

where the  $r_1, r_2, r_3, r_4, s_1, s_2, s_3$  and  $s_4$  are the piecewise functions defined by the followings

$$r_1(r) = \begin{cases} r, & \text{if } \alpha \neq 1 \\ -1, & \text{if } \alpha = 1 \end{cases} \quad (12.a)$$

$$r_2(r) = \begin{cases} r, & \text{if } \alpha \neq 1 \\ 1, & \text{if } \alpha = 1 \end{cases} \quad (12.b)$$

$$r_3(r) = \begin{cases} r, & \text{if } \mu \neq 1 \\ 1, & \text{if } \mu = 1 \end{cases} \quad (12.c)$$

$$r_4(r) = \begin{cases} r, & \text{if } \mu \neq 1 \\ -1, & \text{if } \mu = 1 \end{cases} \quad (12.d)$$

$$s_1(s) = \begin{cases} s, & \text{if } \varepsilon \neq 1 \\ -1, & \text{if } \varepsilon = 1 \end{cases} \quad (12.e)$$

$$s_2(s) = \begin{cases} s, & \text{if } \beta \neq 1 \\ -1, & \text{if } \beta = 1 \end{cases} \quad (12.f)$$

$$s_3(s) = \begin{cases} s, & \text{if } \beta \neq 1 \\ 1, & \text{if } \beta = 1 \end{cases} \quad (12.g)$$

$$s_4(s) = \begin{cases} s, & \text{if } \varepsilon \neq 1 \\ 1, & \text{if } \varepsilon = 1 \end{cases} \quad (12.h)$$

These piecewise functions allow the use of universal serendipity elements as transition elements (Küçükarslan 1995, Utku 2000).

### 3. Formulations of the mass and damping matrices

The formulation for the mass and damping matrices will be presented for the following well-known integrals (Bathe 1995).

$$M_{ij} = \int \rho N_i N_j dA \quad (13)$$

$$C_{ij} = \int \xi N_i N_j dA \quad (14)$$

where  $N_i$  are the shape functions,  $\rho$  and  $\xi$  are the mass density and the damping coefficient per unit area, respectively.

The equation of motion can be written as

$$M\ddot{u} + C\dot{u} + Ku = f(t) \quad (15)$$

where  $M$ ,  $C$  and  $K$  are the global mass, damping and stiffness matrices and  $f(t)$  and  $u$  are the transient load and displacements, respectively. The derivation of the stiffness matrix  $K$  is same as the classical procedure as given in Bathe (1995).

By using the equations from 3 through 11 and substituting these into Eqs. (13) and (14), one can get the mass and damping matrices (Timoshenko and Goodier 1970).

Only for the first row of the mass matrix is given in the followings but one can get the all rows using the Eq. (13).

i) For the mass matrix

$$\begin{aligned}
 M_{11} &= \frac{(2(3 + \varepsilon(3 + 4\varepsilon)) + 2\alpha^2(2 + 5\varepsilon(1 + \varepsilon)) + \alpha(3 + 5\varepsilon(1 + 2\varepsilon)))\rho}{(45(1 + \alpha)^2(1 + \varepsilon)^2)} \\
 M_{12} &= \frac{-5\alpha(\beta - \varepsilon) + 2(-1 + \beta + \varepsilon + \beta\varepsilon) + \alpha^2(4 + 5\varepsilon + 5\beta(1 + 2\varepsilon))\rho}{45(-1 + \alpha^2)(1 + \beta)(1 + \varepsilon)} \\
 M_{13} &= \frac{3 - \varepsilon + \beta(1 + \varepsilon - 5\mu) + \mu + \alpha(-1 + \mu + 5\varepsilon(-1 + \beta\mu))\rho}{45(1 + \alpha)(-1 + \beta)(1 + \varepsilon)(-1 + \mu)} \\
 M_{14} &= \frac{2(-1 + \mu) + \varepsilon(4\varepsilon + 5(-1 + \varepsilon)\mu) + \alpha(2(1 + \mu) + 5\varepsilon(1 + \varepsilon + 2\varepsilon\mu))\rho}{45(1 + \alpha)(-1 + \varepsilon^2)(1 + \mu)} \\
 M_{15} &= -\frac{2(-3 + 2\varepsilon + 5\alpha(1 + 2\varepsilon))\rho}{45(-1 + \alpha)(-1 + \alpha)^2(1 + \varepsilon)} \\
 M_{16} &= -\frac{2(-4 + \alpha + 5\alpha\varepsilon)\rho}{45(1 + \alpha)(-1 + \beta^2)(1 + \varepsilon)} \\
 M_{17} &= -\frac{2(4 + \varepsilon + 5\alpha\varepsilon)\rho}{45(1 + \alpha)(1 + \varepsilon)(-1 + \mu^2)} \\
 M_{18} &= -\frac{2(-3 + 5\varepsilon + 2\alpha(1 + 5\varepsilon))\rho}{45(1 + \alpha)(-1 + \varepsilon)(1 + \varepsilon)^2} \tag{16}
 \end{aligned}$$

ii) For the damping matrix

Since the derivation of the damping is similar to the derivation of the mass matrix, one can write the following

$$C_{ij} = \frac{\xi M_{ij}}{\rho} \text{ and } i, j = 1, 2, \dots, 8 \tag{17}$$

## 4. Numerical examples

### 4.1 Verification example

To examine the validity of the proposed formulations, a concrete cantilever beam (Fig. 4) loaded

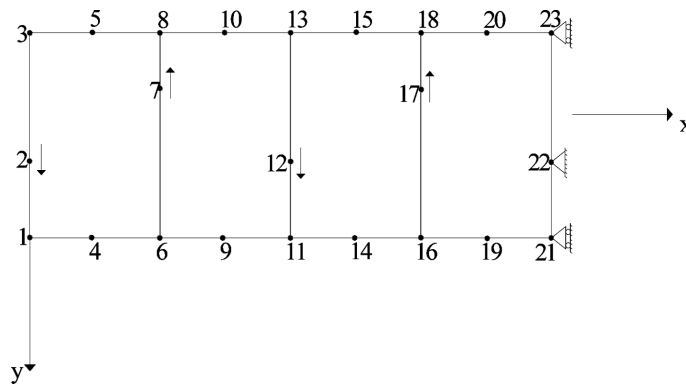


Fig. 4 Cantilever beam ( $E = 20000$  MPa, Poisson's ratio = 0.15, unit weight =  $2400 \text{ kg/m}^3$  and no damping)

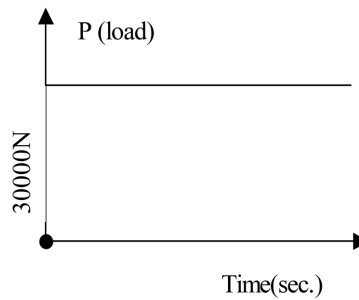


Fig. 5 Heaviside load applied to point 3 in downward direction

with a Heaviside vertical downward load at the tip point (nodal point 3) with the maximum value of 30000 N (Fig. 5). The length of the cantilever is 1200 mm and depth is 300 mm and the thickness is 25 mm. For the analysis, geometrically equal four quadratic elements are used.

The elasticity solution of the vertical displacements of this plane stress problem is given in Timoshenko and Goodier (1970) under static loading by the following formula

$$v = \frac{\nu Pxy^2}{2EI} + \frac{Py^3}{6EI} - \frac{Pl^2x}{2EI} + \frac{Pl^3}{3EI} + \frac{Ph^2(l-x)}{2GI} \tag{18}$$

where  $x$  :  $x$ -coordinate,  $y$  :  $y$ -coordinate,  $P$  : tip load,  $I$  : moment of inertia in the  $z$  direction,  $E$  : modulus of elasticity,  $G$  : shear modulus,  $l$  : length of beam (1200 mm for the example),  $h$  : half depth of the beam (150 mm for the example) and  $\nu$ : Poisson's ratio.

Using the given geometry and the material properties, one can calculate the displacement at the nodal point 3 using the Eq. (18) as  $v_3 = 16.19$  mm. For the finite element analyses, Newmark time integration is used to integrate the Eq. (15) with a time step size of 0.02 seconds. The mesh used in the analysis is given same as in the Fig. 4. For the verification, three different models will be studied. In these models, the mid-points in the vertical direction (nodes 2, 7, 12, 17 and 22) will be shifted first 25 mm, then 50 mm and lastly 75 mm in the shown downward and upward directions, i.e., nodes 7 and 17 are shifted upward and nodes 2, 12 and 22 are shifted downward directions. The analyses are done using by standard and improved shape functions. Standard shape functions are derived for the fixed locations of the edge mid points at the center. Since the mid-points are

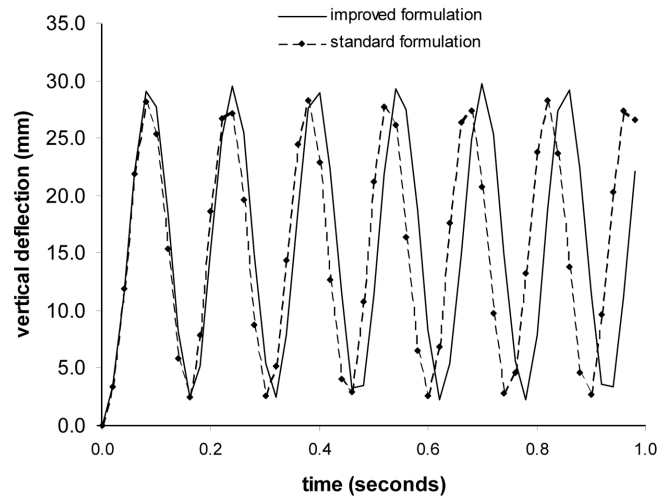


Fig. 6 Time history of the nodal point 3 in the vertical direction for a shift of 25 mm

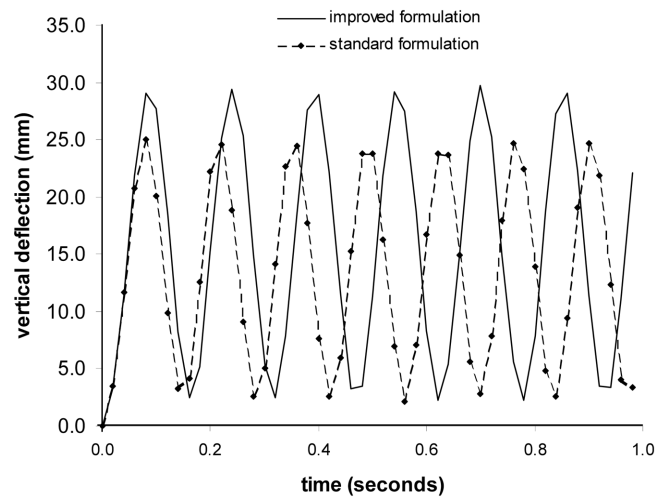


Fig. 7 Time history of the nodal point 3 in the vertical direction for a shift of 50 mm

shifted in the given mesh, standard formulation will produce errors due to mapping distortions.

In the Fig. 6, the results of vertical deflection at node 3 are plotted for 1 second. The average of maximum and minimum peak values of time history of the deflection gives the equivalent value of static loading under the Heaviside loading. From this, the result of the averaged displacement is calculated 15.86 mm and 15.53 mm for improved and standard formulations, respectively.

In the Fig. 7, the results of vertical deflection at node 3 are plotted for 1 second. The result of the averaged displacement is calculated 15.86 mm and 13.62 mm for improved and standard formulations, respectively. Lastly, in the Fig. 8, the time history for a shift amount of 75 mm is plotted. For this case, the result of the averaged displacement is calculated 15.86 mm and 11.64 mm for improved and standard formulations, respectively. As one can observe, the shift of nodes does

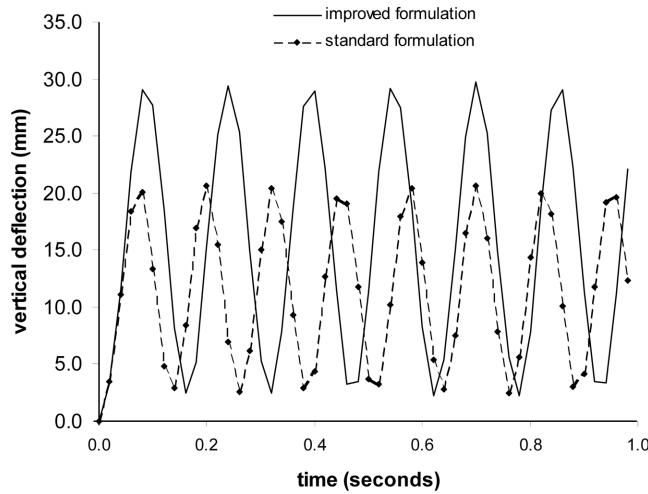


Fig. 8 Time history of the nodal point 3 in vertical direction for a shift of 75 mm

not affect the time history of the node for the improved formulation, but for the standard formulation it does not true. Another observation is the loose of accuracy by increasing the shifting amount for the standard formulation, but for improved one the results are still accurate. The error compared to elasticity solution for improved formulation comes from the number of elements and the method of time integration and the time step size used in the analyses.

#### 4.2 A cantilever beam with a ramp loading and with damping effect

In this section, the same geometry and the same material properties of the example given for verification is used. For this section, only a shift amount of 75 mm is considered, since the highest error occurs in this shift. A damping coefficient of 1% is used and a ramp loading for 0.2 second is applied again on to the nodal point 3 (Fig. 9). The same finite element mesh, the same time integration and time step size are used as in the previous example. With this example, the effect of damping and expected physical behavior was studied for a complete analysis.

In the Figs. 10 and 11, the time history displacement of the node 3 is plotted without damping for vertical and horizontal directions, respectively. In the Figs. 12 and 13, this time same plots are

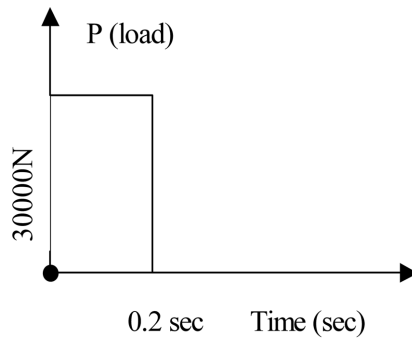


Fig. 9 Transient load applied to point 3 vertically

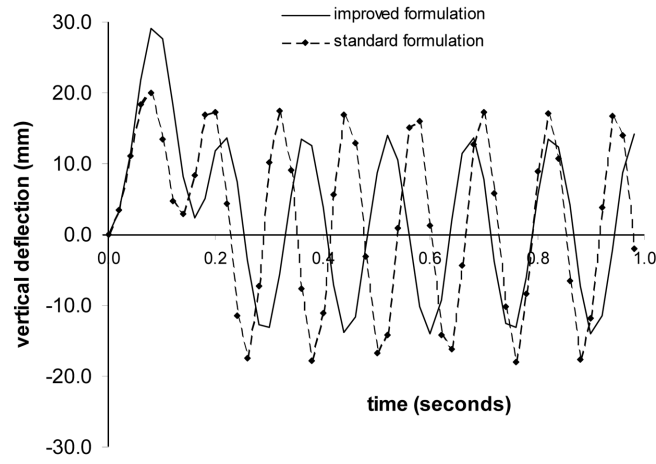


Fig. 10 Time history of the nodal point 3 in the vertical direction without damping

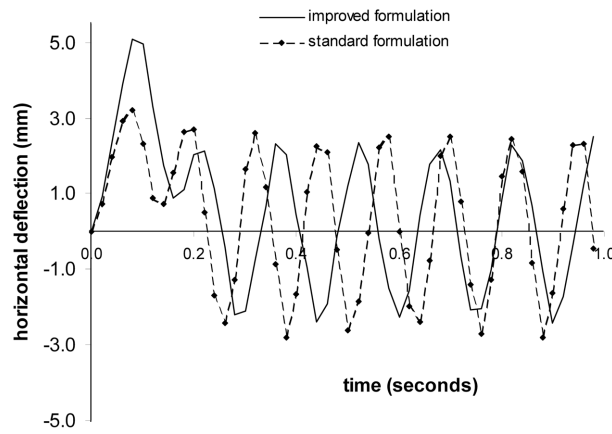


Fig. 11 Time history of the nodal point 3 in the horizontal direction without damping

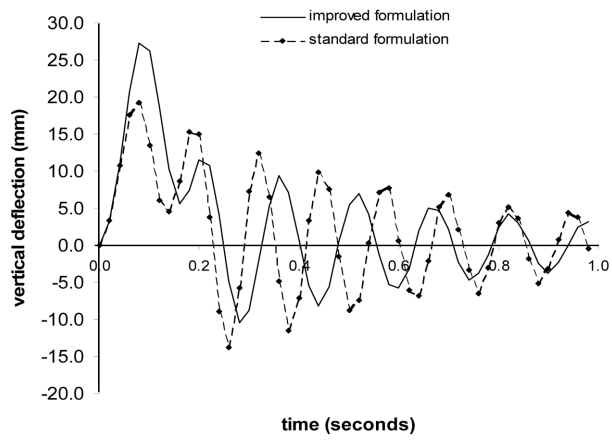


Fig. 12 Time history of the nodal point 3 in the vertical direction with damping

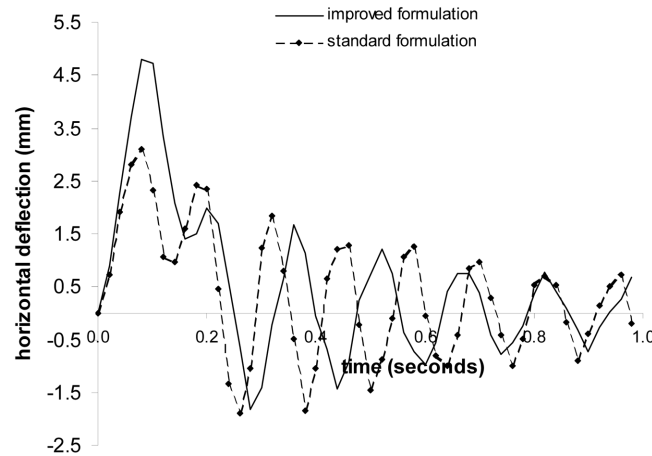


Fig. 13 Time history of the nodal point 3 in horizontal direction with damping

obtained by including the damping. In all these obtained plots, one can observe that, the standard formulation underestimates the positive displacements but overestimates the negative displacements. And also the locations of the results are shifted, i.e., they do not have the same pattern or behavior as in the improved formulation.

## 5. Conclusions

In this paper, a generalization of the concept of the universal serendipity elements (USE) was formulated first time to derive the mass and damping matrices to eliminate mapping distortion errors commonly faced in the dynamical problems. This has been done by using a flexible master element with an adjustable edge node location. The improved formulations gave accurate results for the test problem used in the analyses when compared with the available elasticity results for static analysis. The improved universal serendipity formulation for the mass and damping matrices eliminates the node mapping distortion errors that occurs incase of the standard shape function formulation, and the time history of the results are not properly obtained in the standard formulation due to mapping distortion errors produced for these analyses. The proposed formulation can be used in the any dynamical problems that formulated using by finite element method.

## Acknowledgements

This study was supported by The Scientific and Technological Research Council of Turkey (TÜBİTAK), Engineering Research Group Project Number: MAG-107M316.

## References

Bathe, K.J. (1995), *Finite Element Procedures*, Prentice Hall, NJ.

- Celia, M.A. and Cray, W.G. (1984), "An improved isoparametric transformation for finite element analysis", *Int. J. Numer. Meth. Eng.*, **20**, 1443-1459.
- Chamberland, E., Fortin, A. and Fortin, M. (2010), "Comparison of the performance of some finite element discretizations for large deformation elasticity problems", *Comput. Struct.*, **88**, 664-673.
- Çitıpıtıoğlu, E. (1983), "Universal serendipity elements", *Int. J. Numer. Meth. Eng.*, **19**, 803-810.
- Dhananjaya, H.R., Pandey, P.C. and Nagabhushanam, J. (2009), "New eight node serendipity quadrilateral plate bending element for thin and moderately thick plates using Integrated Force Method", *Struct. Eng. Mech.*, **33**, 485-502.
- Dhananjaya, H.R., Nagabhushanam, J., Pandey, P.C. and Jumaat, M.Z. (2010), "New twelve node serendipity quadrilateral plate bending element based on Mindlin-Reissner theory using Integrated Force Method", *Struct. Eng. Mech.*, **36**, 625-642.
- El-Mezaini, N. and Çitıpıtıoğlu, E. (1991), "Finite element analysis of prestressed and reinforced structures", *J. Struct. Eng.*, **117**, 2851-2864.
- Heng, B.C.P. and Mackie, R.I. (2009), "Using design patterns in object-oriented finite element programming", *Comput. Struct.*, **87**, 952-961.
- Ho, S.P. and Yeh, Y.L. (2006), "The use of 2D enriched elements with bubble functions for finite element analysis", *Comput. Struct.*, **84**, 2081-2091.
- Konstantinos, E., Kakosimos, M. and Assael, J. (2009), "An efficient 3D mesh generator based on geometry decomposition", *Comput. Struct.*, **87**, 27-38.
- Küçükarslan, S. (1995), "Universal serendipity elements with unequally spaced edge nodes", MSc Thesis, METU, Ankara, Turkey.
- Küçükarslan, S. and Demir, A. (2008), "Node mapping correction for universal serendipity element under dynamic loads", *Proceedings of the 4th International Conference on Advances in Structural Engineering and Mechanics*, Jeju, Korea.
- Kikuchi, F., Okabe, M. and Fujio, H. (1999), "Modification of the 8-node serendipity element", *Comput. Meth. Appl. Mech. Eng.*, **179**, 91-109.
- Lim, J.H., Sohn, D., Lee D.H. and Im, S. (2010), "Variable-node finite elements with smoothed integration techniques and their applications for multiscale mechanics problem", *Comput. Struct.*, **88**, 413-425.
- Nicolas, V.T. and Çitıpıtıoğlu, E. (1977), "A general isoparametric finite element program SDRC-SUPERB", *Comput. Struct.*, **7**, 303-313.
- Timoshenko, S.P. and Goodier, J.N. (1970), *Theory of Elasticity*, McGraw Hill, NY.
- Utku, M., Çitıpıtıoğlu, E. and Özkan, G. (1991), "Isoparametric elements with unequally spaced edge nodes", *Comput. Struct.*, **41**, 455-460.
- Utku, M. (2000), "An improved transformation for universal serendipity elements", *Comput. Struct.*, **73**, 199-206.